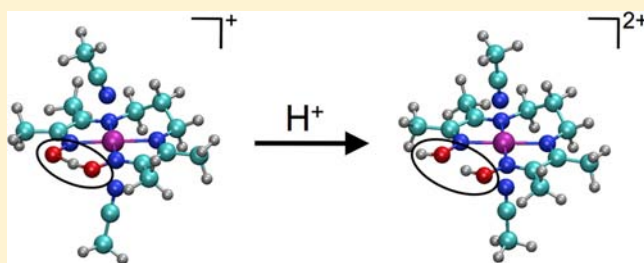


## Effects of Ligand Modification and Protonation on Metal Oxime Hydrogen Evolution Electrocatalysts

Brian H. Solis,<sup>†</sup> Yinxi Yu,<sup>‡</sup> and Sharon Hammes-Schiffer<sup>\*,†</sup><sup>†</sup>Department of Chemistry, 600 South Mathews Avenue, University of Illinois at Urbana–Champaign, Urbana, Illinois 61801, United States<sup>‡</sup>Department of Chemistry, 104 Chemistry Building, Pennsylvania State University, University Park, Pennsylvania 16802, United States

## Supporting Information

**ABSTRACT:** The design of hydrogen-evolving electrocatalysts that operate at modest overpotentials is important for solar energy devices. The  $M^{II/I}$  reduction potential for metal diimine-dioxime and diglyoxime electrocatalysts is often related to the overpotential required for hydrogen evolution. Herein the impact of ligand modification and protonation on the  $M^{II/I}$  reduction potentials for cobalt, nickel, and iron diimine-dioxime and diglyoxime complexes is investigated with computational methods. The calculations are consistent with experimental data available for some of these complexes and additionally provide predictions for complexes that have not yet been synthesized. The calculated  $pK_a$ 's imply that ligand protonation is likely to occur at the O–H–O bridge but not at other ligand sites for these complexes. Moreover, the calculations imply that a ligand-protonated  $Co^{III}$ -hydride intermediate is formed along the  $H_2$  production pathway for catalysts containing an O–H–O bridge in the presence of sufficiently strong acid. The calculated  $M^{II/I}$  reduction potentials indicate that the anodic shift due to protonation of the O–H–O bridge is greater than that due to replacing the O–H–O bridge with an O–BF<sub>2</sub>–O bridge for cobalt and nickel but not for iron complexes. Experiments suggest degradation for complexes with two O–H–O bridges and alternative mechanisms for certain iron complexes with two O–BF<sub>2</sub>–O bridges. Asymmetric cobalt, nickel, and strongly electron withdrawing substituted iron diimine-dioxime and diglyoxime complexes containing a single O–H–O bridge are proposed to be effective hydrogen evolution electrocatalysts with relatively low overpotentials in acetonitrile and water. These insights are important for the design of efficient aqueous-based hydrogen-evolving catalysts.

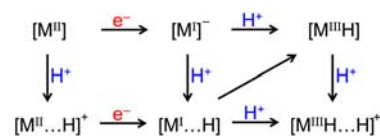


## I. INTRODUCTION

Earth-abundant first-row transition metal complexes are promising catalysts for solar-driven water oxidation and proton reduction.<sup>1</sup> Cobalt diglyoxime catalysts evolve hydrogen in protic solutions both photochemically and electrochemically at modest overpotentials.<sup>2–8</sup> While  $Co(dmgH)_2$  ( $dmg$  = dimethylglyoxime) has been shown to degrade in acidic solutions,<sup>9</sup>  $Co(dmgBF_2)_2$  is much more acid resistant<sup>10</sup> and has been studied extensively.<sup>11–17</sup> Increased stability in acidic solutions can also be achieved by replacing one or both O–H–O bridges of  $Co(dmgH)_2$  with propane,<sup>18</sup> forming the diimine-dioxime complex  $Co(DO)(DOH)pn$  or  $Co(TIM)$ , respectively [ $(DOH)(DOH)pn = N^2,N^{2'}$ -propanediylbis(2,3-butanedione-2-imine-3-oxime) and  $TIM = 2,3,9,10$ -tetramethyl-1,4,8,11-tetraazacyclotetradeca-1,3,8,10-tetraene]. In addition to cobalt complexes, nickel and iron  $H_2$  evolution catalysts have also been studied.<sup>18–21</sup>

Cyclic voltammetry experiments revealed an anodic shift that correlated with acid strength for  $Co(DO)(DOH)pn$  in both water<sup>8</sup> and acetonitrile.<sup>18</sup> In aqueous solution, the Nernstian response of the catalytic peak was ca.  $-60$  mV/pH unit, consistent with a one-electron, one-proton process that was

proposed to involve protonation of the O–H–O bridge.<sup>8</sup> In addition, anodic shifts were observed when the O–H–O bridge was replaced with an O–BF<sub>2</sub>–O bridge in the absence of an acid for cobalt, nickel, and iron complexes.<sup>3,18,21</sup> For complexes without any O–H–O bridges, the Nernstian shift under acidic conditions was no longer observed.<sup>8,18</sup> Scheme 1 depicts the proposed initial steps of the hydrogen production mechanism for cases without ligand protonation (top row) and with ligand protonation (bottom row), where  $M...H$  denotes a ligand-protonated species. Additional steps, such as the reduction of the  $M^{III}$ -hydride to a  $M^{II}$ -hydride, may be required prior to hydrogen production. Understanding the impact of oxime

Scheme 1. Initial Steps of  $H_2$  Evolution Mechanism

Received: February 25, 2013

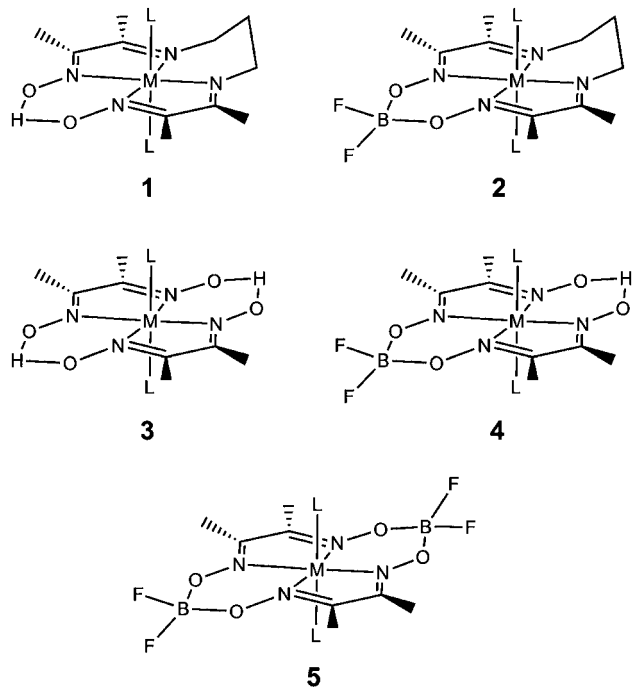
Published: May 23, 2013



bridge modification and protonation is critical for the design of more effective molecular electrocatalysts for H<sub>2</sub> production.

In this paper, we perform a computational investigation of diimine-dioxime (complexes 1–2) and diglyoxime (complexes 3–5) electrocatalysts, as depicted in Chart 1. Some of these

Chart 1. Metal Oxime Complexes



complexes, such as the cobalt and nickel diimine-dioxime complexes,<sup>18</sup> have been studied experimentally. Our calculations are consistent with these previous experimental studies and provide a comprehensive analysis that examines several complexes, such as the asymmetric cobalt diglyoxime complex 4-Co, which have not yet been studied experimentally. Our calculations also provide insight into the physical basis for the observed trends as well as the mechanistic implications. For each complex in Chart 1, we calculate the M<sup>II/I</sup> reduction potential both with and without ligand protonation. This reduction potential often corresponds to the catalytic wave in cyclic voltammetry and therefore is related to the overpotential required for H<sub>2</sub> evolution.<sup>5,13,14,16,18</sup> Thus, a less negative M<sup>II/I</sup> reduction potential typically requires a lower operating potential for these electrocatalysts. Note that under certain conditions, H<sub>2</sub> evolution can occur at the M<sup>III/II</sup>-hydride or M<sup>I/0</sup> potentials, which are not shown in Scheme 1.<sup>17,21</sup> We also calculate the relative pK<sub>a</sub>'s associated with ligand protonation, which leads to an anodic shift of the M<sup>II/I</sup> reduction potential (i.e., the M<sup>II/I</sup>...H potential is less negative than the M<sup>II/I</sup> potential), and the relative pK<sub>a</sub>'s that are associated with forming metal hydrides, which are key intermediates for H<sub>2</sub> production. Consistent with previous experimental studies on some of these complexes,<sup>5,18,21</sup> our calculations indicate that asymmetric cobalt, nickel, and strongly electron withdrawing substituted iron compounds are effective H<sub>2</sub> evolution catalysts.

## II. COMPUTATIONAL METHODS

The computational methods used to calculate reduction potentials and pK<sub>a</sub>'s have been described in detail elsewhere.<sup>16</sup> Each complex was optimized in the gas phase with density functional theory (DFT) with

the B3P86 functional<sup>22,23</sup> and 6-311+G(d,p) basis set<sup>24–28</sup> using Gaussian 09.<sup>29</sup> Gas-phase reaction free energies included both zero point energy and entropic contributions from the vibrational frequencies at T = 298.15 K. Solvation free energies were calculated with the conductor-like polarizable continuum model (C-PCM)<sup>30,31</sup> using Bondi radii<sup>32</sup> and including nonelectrostatic interactions resulting from dispersion,<sup>33,34</sup> repulsion,<sup>34</sup> and cavity formation.<sup>35</sup> The B3P86 functional has been shown to accurately reproduce first-row transition metal complex geometries,<sup>36</sup> and optimizations in the presence of solvent do not significantly affect the geometry. Reduction potentials and pK<sub>a</sub>'s were calculated relative to related, experimentally studied reference complexes to eliminate systematic computational errors arising from limitations in the basis set and exchange-correlation functional.

Benchmarking of this computational procedure has been presented elsewhere,<sup>37–40</sup> including applications to cobaloximes.<sup>16,17</sup> All complexes were calculated as low-spin, as indicated by various experimental analyses.<sup>21,41–44</sup> Optimized gas phase M–N bond lengths are in excellent agreement (within 0.04 Å) with the available crystal structures, as shown in the Supporting Information. Optimizations were performed with two axial solvent ligands for Co<sup>II</sup> and Fe<sup>II</sup>, one solvent ligand for Co<sup>I</sup>, Fe<sup>I</sup>, and Co<sup>III</sup>H, and no solvent ligands for Ni<sup>II</sup> and Ni<sup>I</sup>. These choices were based on the experimental crystal structures<sup>5,8,18,20</sup> and by optimizations of each complex with varying numbers of solvent ligands to determine how many ligands could be bound in stable configurations. Additional computational details are provided in the Supporting Information.

## III. RESULTS AND DISCUSSION

The Co<sup>II/I</sup> reduction potentials calculated in acetonitrile and water are given in Table 1. In acetonitrile, the calculated Co<sup>II/I</sup>

Table 1. Calculated Co<sup>II/I</sup> Reduction Potentials<sup>a</sup>

	E°(Co <sup>II/I</sup> )	E°(Co <sup>II/I</sup> ...H) <sup>b</sup>
	Acetonitrile	
1-Co	–1.11 (–1.11) <sup>c</sup>	–0.73 (ca. –0.78) <sup>d</sup>
2-Co	–0.83 (–0.84)	–0.46
3-Co	–1.43 (–1.48)	–1.11
4-Co	–1.03	–0.71
5-Co	–0.80 (–0.93)	–0.52
	Water	
1-Co	–1.09	–0.70 (–0.70) <sup>c</sup>
2-Co	–0.77	–0.41
4-Co	–1.04	–0.72
5-Co	–0.81 (ca. –0.65)	–0.36

<sup>a</sup>Values given in Volts vs Fc<sup>+</sup>/Fc in acetonitrile and Volts vs SCE in water. Values in parentheses are experimental from ref 18 in acetonitrile and ref 8 in water. <sup>b</sup>Protonation occurs at the O–BF<sub>2</sub>–O bridge for complexes without an O–H–O bridge and at the O–H–O bridge otherwise. <sup>c</sup>E<sub>1/2</sub>(Co<sup>II/I</sup>) for complex 1-Co in acetonitrile [or E<sub>p</sub>(Co<sup>II/I</sup>) in water at pH 1.2] is the reference for complexes in acetonitrile [or water] and agrees with experiment by construction. <sup>d</sup>Experimental value is E<sub>p</sub>(Co<sup>II/I</sup>) with *p*-cyanoanilinium.<sup>18</sup>

reduction potentials are in excellent agreement with the experimental values. In water, the calculated reduction potential of complex 5-Co is in reasonable agreement with the experimental peak potential. Note that some experimental reduction potentials pertain to molecules that were synthesized with different axial ligands, although these ligands are thought to be replaced by solvent ligands in solution. An anodic shift of ~300 mV is observed when the O–H–O bridge is replaced with an O–BF<sub>2</sub>–O or propane bridge in both acetonitrile and water (i.e., 1-Co → 2-Co, 3-Co → 4-Co, 4-Co → 5-Co, 3-Co → 1-Co, 4-Co → 2-Co). In acidic solution, protonation at the

glyoxime bridge also results in an anodic shift in both acetonitrile and water. For all catalysts except complex 3-Co, the Nernstian response due to ligand protonation [i.e.,  $E^{\circ}(\text{Co}^{\text{II}/\text{I}}) \rightarrow E^{\circ}(\text{Co}^{\text{II}/\text{I}}\dots\text{H})$  in Table 1] is slightly greater than the effect of modifying the oxime bridge. Figure 1 depicts the structural changes that occur upon ligand protonation and reduction of complex 1-Co.

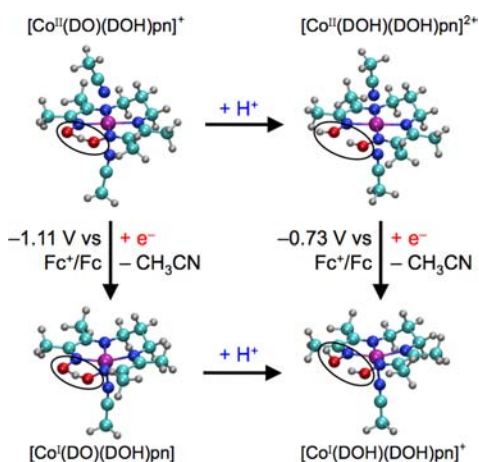


**Figure 1.** Gas phase optimized Co(DO)(DOH)pn complex (1-Co) with and without ligand protonation for the oxidized and reduced states. The O–H–O bridge is circled for clarity.

We calculated the  $pK_a$ 's associated with protonation of the ligand or protonation at the  $\text{Co}^{\text{I}}$  center to form a  $\text{Co}^{\text{III}}$ -hydride species. The former are denoted "ligand  $pK_a$ 's" ( $\text{Co}\dots\text{H}$ ), and the latter are denoted "metal  $pK_a$ 's" ( $\text{CoH}$ ). Figure 2 depicts these  $pK_a$ 's in acetonitrile relative to the ligand  $pK_a$  of complex 1-Co, which has been shown to exhibit a Nernstian response in the presence of certain acids in acetonitrile and water.<sup>8,18</sup> In acetonitrile, complex 1-Co exhibits a Nernstian shift in the presence of anilinium tetrafluoroborate ( $pK_a = 10.7$ ), but not in the presence of trifluoroacetic acid ( $pK_a = 12.7$ ),<sup>18</sup> suggesting that the  $pK_a$  of zero in Figure 2 is in the range of 10.7–12.7  $pK_a$  units in acetonitrile.

For ligand protonation, the  $pK_a$ 's were calculated by adding a proton to the O–H–O bridge of complexes 1-Co, 3-Co, and 4-Co and to the O–BF<sub>2</sub>–O bridge of complexes 2-Co and 5-Co. Qualitatively, a larger relative  $pK_a$  corresponds to a greater thermodynamic probability of ligand protonation by a specified acid. Thus, positive relative  $pK_a$ 's indicate that ligand protonation by an acid that is known to protonate reference complex 1-Co (i.e., an acid with  $pK_a \leq 10.7$  in acetonitrile) is thermodynamically favorable. Compounds with slightly negative relative  $pK_a$ 's can still become protonated, as long as a strong enough acid is used. The extremely negative values of the calculated relative  $pK_a$ 's for ligand protonation of complexes 2-Co and 5-Co suggest that protonation at the O–BF<sub>2</sub>–O bridge is significantly less thermodynamically favorable than protonation at the O–H–O bridge of complex 1-Co both before (black lines in Figure 2) and after (blue lines) reduction. These values are consistent with experiments that indicate a lack of a Nernstian shift for complexes 2-Co and 5-Co in the presence of *p*-cyanoanilinium ( $pK_a = 7.6$ ) and tosic acid ( $pK_a \sim 8.4$ ) in acetonitrile.<sup>5,18</sup> Protonation of complex 1-Co at the oxime nitrogen (lower purple line) or the imine nitrogen (upper purple line) is also thermodynamically less favorable in acetonitrile, consistent with the cyclic voltammograms of

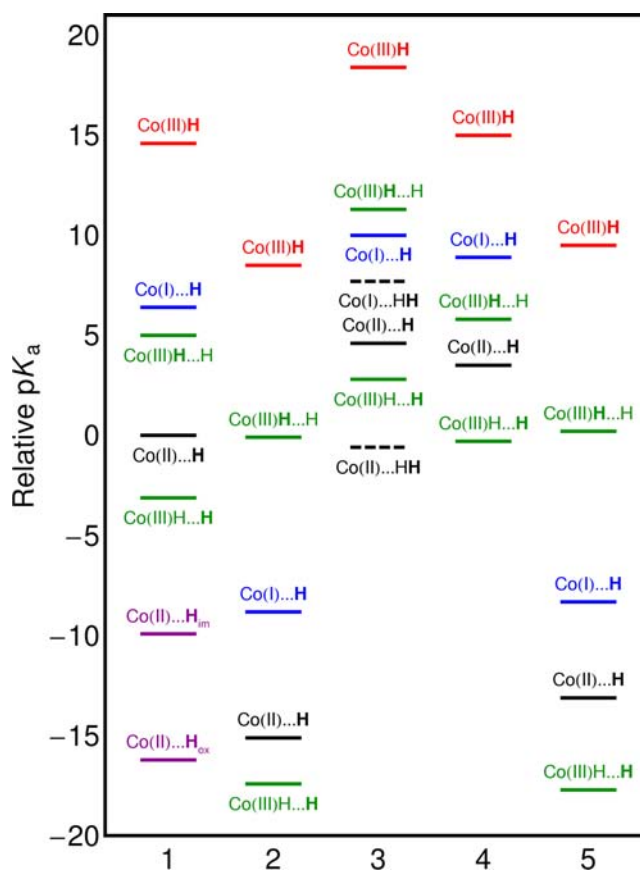


**Figure 2.** Calculated  $pK_a$ 's of cobalt complexes in acetonitrile relative to the  $pK_a$  of ligand-protonated 1-Co. The bold H is the proton removed to calculate the  $pK_a$ . Ligand protonation is denoted  $\text{Co}\dots\text{H}$ , and protonation at the metal center to form a metal hydride is denoted  $\text{CoH}$ . Ligand protonation occurs at the O–H–O bridge for complexes 1-Co, 3-Co, and 4-Co and at the O–BF<sub>2</sub>–O bridge for complexes 2-Co and 5-Co, except where specified otherwise. Experimental studies<sup>18</sup> suggest that zero relative  $pK_a$  in this figure corresponds to a value in the range of 10.7–12.7  $pK_a$  units in acetonitrile. For complexes 1-Co and 4-Co, the  $\text{Co}^{\text{II}}$  species is expected to have a protonated ligand prior to reduction (black lines), followed by protonation of the ligand-protonated  $\text{Co}^{\text{I}}$  species (blue lines) at the metal center to form the ligand-protonated  $\text{Co}^{\text{III}}$ -hydride species (upper green lines). For complexes 2-Co and 5-Co, the  $\text{Co}^{\text{II}}$  species is not expected to have a protonated ligand prior to or subsequent to  $\text{Co}^{\text{II}/\text{I}}$  reduction, leading to the  $\text{Co}^{\text{III}}$ -hydride species without ligand protonation (red lines). Complex 3-Co is not stable in acidic solution, most likely due to double ligand protonation (dashed black lines). Expanded version provided in the Supporting Information.

methyl-substituted Co(TIM) that showed no Nernstian shift in the presence of tosic acid.<sup>5</sup> Calculated  $pK_a$ 's in water are qualitatively similar and are depicted in an expanded version of Figure 2 in the Supporting Information.

We also considered the possibility of protonation at both O–H–O bridges for complex 3-Co. The relative  $pK_a$ 's for the second ligand protonation of complex 3-Co in acetonitrile are  $-0.6$  for  $\text{Co}^{\text{II}}$  (lower dashed line in Figure 2) and  $7.7$  for  $\text{Co}^{\text{I}}$  (upper dashed line), suggesting that ligand protonation is thermodynamically favorable at both O–H–O bridges by an acid known to protonate reference complex 1-Co. For this doubly protonated species, the  $\text{Co}^{\text{II}/\text{I}}$  reduction potential is  $-0.63$  V vs  $\text{Fc}^+/\text{Fc}$  in acetonitrile, which is more positive than the value for the singly protonated species ( $-1.11$  V vs  $\text{Fc}^+/\text{Fc}$

in acetonitrile). Thus, the calculations predict that protonation of both O–H–O bridges would lead to a significantly greater anodic shift than observed for the singly protonated species (i.e., 800 mV vs 300 mV). However, experimental evidence suggests that diglyoximes with two O–H–O bridges degrade in acidic solution, possibly due to weakening of the hydrogen bonding in the glyoximate macrocycle. Note that even under neutral or basic pH conditions, photochemical experiments of cobaloximes with two dmGH ligands undergo decomposition, suggesting that alternative degradation pathways exist.<sup>45–47</sup> Therefore, asymmetric cobalt complexes with a single O–H–O bridge are predicted to be effective and stable electrocatalysts.

We also calculated the metal  $pK_a$ 's that are associated with protonation at the  $\text{Co}^{\text{I}}$  center to form a  $\text{Co}^{\text{III}}$ -hydride species, both with and without the ligand protonated. The metal  $pK_a$ 's of the  $\text{Co}^{\text{III}}$ -hydrides without ligand protonation (red lines in Figure 2) are greater than the ligand  $pK_a$ 's of the ligand-protonated  $\text{Co}^{\text{I}}$  species (blue lines), indicating that an intramolecular proton transfer from the oxime bridge to the metal center is thermodynamically favorable (i.e., the diagonal arrow in Scheme 1). However, this intramolecular proton transfer may be hindered by a large energy barrier, although nearby solvent molecules could potentially assist in the proton transfer mechanism. Moreover, the relative  $pK_a$  for ligand protonation of the  $\text{Co}^{\text{III}}$ -hydride (i.e.,  $\text{Co}^{\text{III}}\text{H}\dots\text{H}$ , lower green lines in Figure 2) is  $-3.1$  for complex **1-Co** and  $-0.3$  for complex **4-Co**, suggesting that the ligand-protonated  $\text{Co}^{\text{III}}$ -hydride species could form after intramolecular proton transfer. Alternatively, the relative metal  $pK_a$ 's of the ligand-protonated  $\text{Co}^{\text{III}}$ -hydride species (i.e.,  $\text{Co}^{\text{III}}\text{H}\dots\text{H}$ , upper green lines in Figure 2) are positive, signifying that the metal center of the ligand-protonated species could also be protonated directly by an acid in solution known to protonate the reference complex **1-Co**. Overall, these calculations predict that a ligand-protonated  $\text{Co}^{\text{III}}$ -hydride intermediate will be formed along the  $\text{H}_2$  production pathway in the presence of sufficiently strong acids for complexes **1-Co** and **4-Co**.

While the relative metal  $pK_a$ 's of the ligand-protonated  $\text{Co}^{\text{III}}$ -hydride species (upper green lines in Figure 2) of complexes **2-Co** and **5-Co**, are positive, these species are unlikely to form in solution. Experiments indicate that the  $\text{Co}^{\text{II}}$  species are not protonated for these complexes, so  $\text{Co}^{\text{I}}\dots\text{H}$  is not generated by the electrochemical  $\text{Co}^{\text{II/I}}$  reduction.<sup>5,18</sup> Formation of  $\text{Co}^{\text{III}}\text{H}$  (red lines) is much more thermodynamically favorable than formation of  $\text{Co}^{\text{I}}\dots\text{H}$  (blue lines), indicating that  $\text{Co}^{\text{III}}\text{H}$  will form preferentially over  $\text{Co}^{\text{I}}\dots\text{H}$  after reduction. Furthermore, ligand protonation after the formation of  $\text{Co}^{\text{III}}\text{H}$  is associated with extremely negative relative  $pK_a$ 's for complexes **2-Co** and **5-Co** (lower green lines). Thus, for complexes **2-Co** and **5-Co** these calculations predict that  $\text{H}_2$  evolution will proceed through a  $\text{Co}^{\text{III}}$ -hydride without ligand protonation under typical experimental conditions. For all complexes studied, the  $\text{Co}^{\text{III}}$ -hydride species can produce hydrogen bimetallically or monometallically, and in many cases, it may be further reduced to a  $\text{Co}^{\text{II}}$ -hydride species prior to hydrogen evolution.<sup>14–16</sup>

To investigate the impact of the metal center on these trends, we calculated the  $\text{Fe}^{\text{II/I}}$  and  $\text{Ni}^{\text{II/I}}$  reduction potentials in acetonitrile, as given in Table 2. The calculated anodic shift of the  $\text{Ni}^{\text{II/I}}$  reduction potential upon replacing the O–H–O bridge in complex **1-Ni** with O–BF<sub>2</sub>–O (i.e., **1-Ni** → **2-Ni**) is 360 mV, which is in qualitative agreement with the experimentally observed shift of 250 mV for this catalyst.<sup>18</sup> The analogous calculated anodic shift for complex **4-Ni** (i.e., **4-**

**Table 2.** Calculated  $\text{Fe}^{\text{II/I}}$  and  $\text{Ni}^{\text{II/I}}$  Reduction Potentials<sup>a</sup>

	$E^\circ(\text{Fe}^{\text{II/I}})$	$E^\circ(\text{Fe}^{\text{II/I}}\dots\text{H})^b$
<b>1-Fe</b>	–2.64	–2.22
<b>2-Fe</b>	–2.02	N/A
<b>5-Fe</b>	–2.13 (ca. –2.13) <sup>c</sup>	N/A
	$E^\circ(\text{Ni}^{\text{II/I}})$	$E^\circ(\text{Ni}^{\text{II/I}}\dots\text{H})^b$
<b>1-Ni</b>	–1.22 (–1.22) <sup>c</sup>	–0.59 (ca. –0.95) <sup>d</sup>
<b>2-Ni</b>	–0.86 (–0.97)	N/A
<b>4-Ni</b>	–1.29	–0.59
<b>5-Ni</b>	–0.97	N/A

<sup>a</sup>Values given in Volts vs  $\text{Fc}^+/\text{Fc}$  in acetonitrile. Values in parentheses are experimental from ref 20 (shifted from SCE with  $-0.38\text{ V}$ )<sup>48</sup> for Fe and ref 18 for Ni. <sup>b</sup>Protonation occurs at the O–H–O bridge. <sup>c</sup> $E_{1/2}(\text{M}^{\text{II/I}})$  for complexes **5-Fe** and **1-Ni** in acetonitrile were the references for Fe and Ni complexes, respectively, and agree with experiment by construction. <sup>d</sup>Experimental value is  $E_p(\text{Ni}^{\text{II/I}})$  with three equivalents of *p*-cyanoanilinium.<sup>18</sup>

**Ni** → **5-Ni**) is of similar magnitude, but this species has not been studied experimentally. The calculated  $\text{Fe}^{\text{II/I}}$  reduction potential shifts 620 mV anodically when the O–H–O bridge of complex **1-Fe** is replaced with an O–BF<sub>2</sub>–O bridge (i.e., **1-Fe** → **2-Fe**). This shift is in good agreement with the  $\sim 640$  mV anodic shift in the  $\text{Fe}^{\text{II/I}}$  couple observed in cyclic voltammetry when the O–H–O bridge of  $\text{Fe}(\text{dAr}^{\text{F}}\text{g}_2\text{H}-\text{BF}_2)$  ( $\text{dAr}^{\text{F}}\text{g}$  = dipentafluorophenylglyoxime) is replaced with O–BF<sub>2</sub>–O.<sup>21</sup>

In terms of ligand protonation, the calculations indicate that protonation of the O–H–O bridge results in a 420 mV anodic shift of the  $\text{Fe}^{\text{II/I}}$  reduction potential for complex **1-Fe** and an average 665 mV anodic shift of the  $\text{Ni}^{\text{II/I}}$  reduction potential for complexes **1-Ni** and **4-Ni**. The calculated  $\text{Ni}^{\text{II/I}}$  reduction potential of ligand-protonated complex **1-Ni** is 360 mV more positive than the experimental peak potential in the presence of three equivalents of *p*-cyanoanilinium,<sup>18</sup> suggesting that the complex requires a stronger acid for complete ligand protonation. In contrast to the nickel and cobalt complexes, the anodic shift of the  $\text{Fe}^{\text{II/I}}$  reduction potential due to ligand protonation of complex **1-Fe** is less than the anodic shift due to replacement of the O–H–O bridge with O–BF<sub>2</sub>–O (420 mV vs 620 mV shift). This trend is also observed experimentally for the  $\text{Fe}^{\text{II/I}}$  reduction potentials of  $\text{Fe}(\text{dAr}^{\text{F}}\text{g}_2\text{H}-\text{BF}_2)$  and  $\text{Fe}(\text{dAr}^{\text{F}}\text{gBF}_2)_2$ .<sup>21</sup>

Typically iron diimine-dioxime and diglyoxime electrocatalysts require large overpotentials, rendering these catalysts ineffective for  $\text{H}_2$  production. Of the iron complexes studied herein, complex **2-Fe** has the least negative  $\text{Fe}^{\text{II/I}}$  potential at  $-2.02\text{ V}$  vs  $\text{Fc}^+/\text{Fc}$ , which requires more than an additional volt of overpotential compared to effective cobaloxime electrocatalysts. Previously, Rose et al. showed that the strongly electron withdrawing substituents of  $\text{Fe}(\text{dAr}^{\text{F}}\text{gBF}_2)_2$  and  $\text{Fe}(\text{dAr}^{\text{F}}\text{g}_2\text{H}-\text{BF}_2)$  lead to operating potentials of  $-0.9$  and  $-0.8\text{ V}$  vs SCE, respectively, in  $\text{CH}_2\text{Cl}_2$ .<sup>21</sup> In this case, the asymmetric  $\text{Fe}(\text{dAr}^{\text{F}}\text{g}_2\text{H}-\text{BF}_2)$  operates at a more positive potential than  $\text{Fe}(\text{dAr}^{\text{F}}\text{gBF}_2)_2$  because it catalyzes  $\text{H}_2$  through a different mechanism. The substituents are so strongly electron withdrawing in  $\text{Fe}(\text{dAr}^{\text{F}}\text{gBF}_2)_2$  that the catalytic peak is identified as the  $\text{Fe}^{\text{I/0}}$  couple, presumably because the  $\text{Fe}^{\text{I}}$  complex cannot become protonated to form an  $\text{Fe}^{\text{III}}$ -hydride. According to this analysis, the replacement of one O–BF<sub>2</sub>–O bridge with an O–H–O bridge decreases the ligand electron withdrawing effect enough that  $\text{Fe}^{\text{I}}$  can become protonated, thus allowing  $\text{Fe}(\text{dAr}^{\text{F}}\text{g}_2\text{H}-\text{BF}_2)$  to catalyze  $\text{H}_2$  evolution at the

more positive  $\text{Fe}^{\text{II/I}}$  couple. Therefore, asymmetric iron complexes with strongly electron withdrawing substituents are also effective  $\text{H}_2$  evolution electrocatalysts. Note that while complex **5-Fe** has been characterized experimentally,<sup>20</sup> complexes **3-Fe** and **4-Fe**, with one or two O–H–O bridges, have not been synthesized and may not be stable without strongly electron withdrawing substituents.

#### IV. CONCLUSION

In this paper, we examined the impact of ligand modification and protonation on the  $\text{M}^{\text{II/I}}$  reduction potentials for cobalt, nickel, and iron diimine-dioxime and diglyoxime complexes. Our objective was to identify catalysts with a less negative  $\text{M}^{\text{II/I}}$  reduction potential, which typically determines the required overpotential for  $\text{H}_2$  evolution. The anodic shift of the  $\text{M}^{\text{II/I}}$  reduction potential is greater upon protonation of the O–H–O bridge than upon replacement of an O–H–O bridge with the more electron withdrawing O–BF<sub>2</sub>–O or propane bridge for cobalt and nickel complexes, but the opposite trend is observed for iron complexes. These results suggest that the optimal cobalt and nickel catalysts have two O–H–O bridges, while the optimal iron catalysts have O–BF<sub>2</sub>–O and propane bridges. Catalysts with two O–H–O bridges have been found to degrade in acidic solution, however, suggesting that the optimal cobalt and nickel catalysts are asymmetric with a single O–H–O bridge. Asymmetric iron complexes with a single O–H–O bridge and strongly electron withdrawing substituents are also expected to catalyze  $\text{H}_2$  evolution at less negative potentials than those with two O–BF<sub>2</sub>–O or propane bridges but for a different reason. Strongly electron withdrawing substituents allow iron complexes to operate at modest potentials but can lead to a different mechanism in which the required overpotential is determined by the  $\text{Fe}^{\text{I/0}}$  instead of the  $\text{Fe}^{\text{II/I}}$  reduction potential. Limiting the ligand electron withdrawing effect by synthesizing iron complexes with a single O–H–O bridge can retain the original mechanism and thus lead to a lower required overpotential.

The calculations also provided insight into aspects of the hydrogen production mechanism for the various complexes. Specifically, the calculated relative  $\text{p}K_{\text{a}}$ 's associated with protonation of the ligand or protonation at the  $\text{Co}^{\text{I}}$  metal center to form a  $\text{Co}^{\text{III}}$ -hydride identified the thermodynamically preferred pathways. In the presence of sufficiently strong acids, complexes **1-Co** and **4-Co** are expected to follow the lower pathway in Scheme 1, starting with a ligand-protonated  $\text{Co}^{\text{II}}$  species, followed by reduction to the ligand-protonated  $\text{Co}^{\text{I}}$  species, followed by either intramolecular proton transfer to the metal center (diagonal arrow), which may be prohibited by a high barrier, or proton transfer from an acid directly to the metal center (horizontal arrow), leading to a  $\text{Co}^{\text{III}}$ -hydride species that is likely ligand-protonated. Under similar acidic conditions, complexes **2-Co** and **5-Co** are expected to follow the upper pathway in Scheme 1, starting with  $\text{Co}^{\text{II/I}}$  reduction without ligand protonation, followed by protonation at the metal center to form the  $\text{Co}^{\text{III}}$ -hydride species, which is unlikely to be ligand-protonated. In all of these schemes, the  $\text{Co}^{\text{III}}$ -hydride species may be further reduced to a  $\text{Co}^{\text{II}}$ -hydride species prior to hydrogen evolution.

These results indicate that asymmetric cobalt, nickel, and strongly electron withdrawing substituted (e.g., highly fluorinated) iron complexes with a single O–H–O bridge will be effective hydrogen evolution electrocatalysts. Calculations of cobalt complexes in water show similar trends as in acetonitrile.

The predictions generated from this study of O–H–O bridge modification and protonation, together with our previous study on electron withdrawing substituents,<sup>17</sup> can be used to tune the reduction potentials of these electrocatalysts. These insights are important for the design of efficient, aqueous-based hydrogen-evolving catalysts with minimal required overpotentials.

#### ■ ASSOCIATED CONTENT

##### Supporting Information

Discussion of optimized geometries; selected optimized bond lengths; calculated relative  $\text{p}K_{\text{a}}$ 's; expanded Figure 2; coordinates and energies of optimized structures. This material is available free of charge via the Internet at <http://pubs.acs.org>.

#### ■ AUTHOR INFORMATION

##### Corresponding Author

\*E-mail: [shs3@illinois.edu](mailto:shs3@illinois.edu).

##### Notes

The authors declare no competing financial interest.

#### ■ ACKNOWLEDGMENTS

We thank Michael Rose, Christopher Uyeda, and Samantha Horvath for helpful discussion and input. This work was supported by the NSF Center for Chemical Innovation (Powering the Planet, grant CHE-0802907).

#### ■ REFERENCES

- (1) Du, P.; Eisenberg, R. *Energy Environ. Sci.* **2012**, *5*, 6012–6021.
- (2) Connolly, P.; Espenson, J. H. *Inorg. Chem.* **1986**, *25*, 2684–2688.
- (3) Razavet, M.; Artero, V.; Fontecave, M. *Inorg. Chem.* **2005**, *44*, 4786–4795.
- (4) Hu, X.; Cossairt, B. M.; Brunschwig, B. S.; Lewis, N. S.; Peters, J. C. *Chem. Commun.* **2005**, 4723–4725.
- (5) Hu, X.; Brunschwig, B. S.; Peters, J. C. *J. Am. Chem. Soc.* **2007**, *129*, 8988–8998.
- (6) Baffert, C.; Artero, V.; Fontecave, M. *Inorg. Chem.* **2007**, *46*, 1817–1824.
- (7) Dempsey, J. L.; Brunschwig, B. S.; Winkler, J. R.; Gray, H. B. *Acc. Chem. Res.* **2009**, *42*, 1995–2004.
- (8) McCrory, C. C. L.; Uyeda, C.; Peters, J. C. *J. Am. Chem. Soc.* **2012**, *134*, 3164–3170.
- (9) Gjerde, H. B.; Espenson, J. H. *Organometallics* **1982**, *1*, 435–440.
- (10) Bakac, A.; Espenson, J. H. *J. Am. Chem. Soc.* **1984**, *106*, 5197–5202.
- (11) Du, P.; Schneider, J.; Luo, G.; Brennessel, W. W.; Eisenberg, R. *Inorg. Chem.* **2009**, *48*, 4952–4962.
- (12) Szajna-Fuller, E.; Bakac, A. *Eur. J. Inorg. Chem.* **2010**, 2488–2494.
- (13) Dempsey, J. L.; Winkler, J. R.; Gray, H. B. *J. Am. Chem. Soc.* **2010**, *132*, 1060–1065.
- (14) Dempsey, J. L.; Winkler, J. R.; Gray, H. B. *J. Am. Chem. Soc.* **2010**, *132*, 16774–16776.
- (15) Muckerman, J. T.; Fujita, E. *Chem. Commun.* **2011**, *47*, 12456–12458.
- (16) Solis, B. H.; Hammes-Schiffer, S. *Inorg. Chem.* **2011**, *50*, 11252–11262.
- (17) Solis, B. H.; Hammes-Schiffer, S. *J. Am. Chem. Soc.* **2011**, *133*, 19036–19039.
- (18) Jacques, P.-A.; Artero, V.; Pécaut, J.; Fontecave, M. *Proc. Natl. Acad. Sci. U.S.A.* **2009**, *106*, 20627–20632.
- (19) Pantani, O.; Anxolabéhère-Mallart, E.; Aukauloo, A.; Millet, P. *Electrochem. Commun.* **2007**, *9*, 54–58.
- (20) Rose, M. J.; Winkler, J. R.; Gray, H. B. *Inorg. Chem.* **2012**, *51*, 1980–1982.
- (21) Rose, M. J.; Gray, H. B.; Winkler, J. R. *J. Am. Chem. Soc.* **2012**, *134*, 8310–8313.

- (22) Becke, A. D. *J. Chem. Phys.* **1993**, *98*, 5648–5652.
- (23) Perdew, J. P. *Phys. Rev. B* **1986**, *33*, 8822–8824.
- (24) Wachters, A. J. H. *J. Chem. Phys.* **1970**, *52*, 1033–1036.
- (25) McLean, A. D.; Chandler, G. S. *J. Chem. Phys.* **1980**, *72*, 5639–5648.
- (26) Krishnan, R.; Binkley, J. S.; Seeger, R.; Pople, J. A. *J. Chem. Phys.* **1980**, *72*, 650–654.
- (27) Hay, P. J. *J. Chem. Phys.* **1977**, *66*, 4377–4384.
- (28) Raghavachari, K.; Trucks, G. W. *J. Chem. Phys.* **1989**, *91*, 1062–1065.
- (29) Frisch, M. J.; Trucks, G. W.; Schlegel, H. B.; Scuseria, G. E.; Robb, M. A.; Cheeseman, J. R.; Scalmani, G.; Barone, V.; Mennucci, B.; Petersson, G. A.; Nakatsuji, H.; Caricato, M.; Li, X.; Hratchian, H. P.; Izmaylov, A. F.; Bloino, J.; Zheng, G.; Sonnenberg, J. L.; Hada, M.; Ehara, M.; Toyota, K.; Fukuda, R.; Hasegawa, J.; Ishida, M.; Nakajima, T.; Honda, Y.; Kitao, O.; Nakai, H.; Vreven, T.; Montgomery, J. A., Jr.; Peralta, J. E.; Ogliaro, F.; Bearpark, M.; Heyd, J. J.; Brothers, E.; Kudin, K. N.; Staroverov, V. N.; Kobayashi, R.; Normand, J.; Raghavachari, K.; Rendell, A.; Burant, J. C.; Iyengar, S. S.; Tomasi, J.; Cossi, M.; Rega, N.; Millam, J. M.; Klene, M.; Knox, J. E.; Cross, J. B.; Bakken, V.; Adamo, C.; Jaramillo, J.; Gomperts, R.; Stratmann, R. E.; Yazyev, O.; Austin, A. J.; Cammi, R.; Pomelli, C.; Ochterski, J. W.; Martin, R. L.; Morokuma, K.; Zakrzewski, V. G.; Voth, G. A.; Salvador, P.; Dannenberg, J. J.; Dapprich, S.; Daniels, A. D.; Farkas, Ö.; Foresman, J. B.; Ortiz, J. V.; Cioslowski, J.; Fox, D. J. *Gaussian 09*, revision C.1; Gaussian, Inc.: Wallingford, CT, 2009.
- (30) Barone, V.; Cossi, M. *J. Phys. Chem. A* **1998**, *102*, 1995–2001.
- (31) Cossi, M.; Rega, N.; Scalmani, G.; Barone, V. *J. Comput. Chem.* **2003**, *24*, 669–681.
- (32) Bondi, A. *J. Phys. Chem.* **1964**, *68*, 441–451.
- (33) Floris, F.; Tomasi, J. *J. Comput. Chem.* **1989**, *10*, 616–627.
- (34) Floris, F. M.; Tomasi, J.; Ahuir, J. L. P. *J. Comput. Chem.* **1991**, *12*, 784–791.
- (35) Pierotti, R. A. *Chem. Rev.* **1976**, *76*, 717–726.
- (36) Niu, S.; Hall, M. B. *Chem. Rev.* **2000**, *100*, 353–405.
- (37) Qi, X.-J.; Fu, Y.; Liu, L.; Guo, Q.-X. *Organometallics* **2007**, *26*, 4197–4203.
- (38) Chen, S.; Rousseau, R.; Raugei, S.; Dupuis, M.; DuBois, D. L.; Bullock, R. M. *Organometallics* **2011**, *30*, 6108–6118.
- (39) Fernandez, L. E.; Horvath, S.; Hammes-Schiffer, S. *J. Phys. Chem. C* **2012**, *116*, 3171–3180.
- (40) Fernandez, L. E.; Horvath, S.; Hammes-Schiffer, S. *J. Phys. Chem. Lett.* **2013**, *4*, 542–546.
- (41) Lovecchio, F. V.; Gore, E. S.; Busch, D. H. *J. Am. Chem. Soc.* **1974**, *96*, 3109–3118.
- (42) Gagné, R. R.; Spiro, C. L. *J. Am. Chem. Soc.* **1980**, *102*, 1444–1446.
- (43) Gagné, R. R.; Ingle, D. M. *Inorg. Chem.* **1981**, *20*, 420–425.
- (44) Thompson, D. W.; Stynes, D. V. *Inorg. Chem.* **1990**, *29*, 3815–3822.
- (45) Fihri, A.; Artero, V.; Razavet, M.; Baffert, C.; Leibl, W.; Fontecave, M. *Angew. Chem., Int. Ed.* **2008**, *47*, 564–567.
- (46) Probst, B.; Kolano, C.; Hamm, P.; Alberto, R. *Inorg. Chem.* **2009**, *48*, 1836–1843.
- (47) Probst, B.; Rodenberg, A.; Guttentag, M.; Hamm, P.; Alberto, R. *Inorg. Chem.* **2010**, *49*, 6453–6460.
- (48) Pavlishchuk, V. V.; Addison, A. W. *Inorg. Chim. Acta* **2000**, *298*, 97–102.